Article

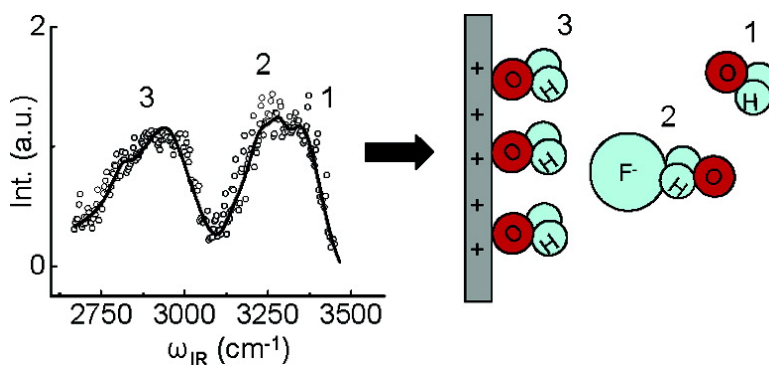# Potential Dependent Organization of Water at the Electrified Metal–Liquid Interface

Zachary D. Schultz, Scott K. Shaw, and Andrew A. Gewirth

More About This Article

Additional resources and features associated with this article are available within the HTML version:

- Supporting Information
- Links to the 8 articles that cite this article, as of the time of this article download
- Access to high resolution figures
- Links to articles and content related to this article
- Copyright permission to reproduce figures and/or text from this article

View the Full Text HTML

Potential Dependent Organization of Water at the Electrified Metal−Liquid Interface

Zachary D. Schultz, Scott K. Shaw, and Andrew A. Gewirth*

Contribution from the Department of Chemistry and Frederick Seitz Materials Research Laboratory, University of Illinois at Urbana−Champaign, Urbana, Illinois 61801

Received June 30, 2005; E-mail: agewirth@uiuc.edu

Abstract: In situ infrared visible sum frequency generation spectroscopy (SFG) is used to examine the structure of water at the Ag−water interface in NaF and KF electrolyte solutions. Water is observed in environments associated with both the electrode surface and the diffuse double layer. Peaks are observed that are correlated with low-order water, water interacting with electrolyte ions, specifically adsorbed water to the electrode surface, and hydronium. Spectra obtained from a thiol-modified Ag surface enabled discrimination between surface-bound water and that in the double layer. The water organization is dependent on applied potential, with the observed intensities for specifically adsorbed and ion solvating water diminishing near the pzc.

1. Introduction

The structure of water at the electrified metal−liquid interface influences electrochemical reactivity in ways important to fields as diverse as corrosion, electrodeposition, and fuel cells.[1] There are numerous studies examining the structure of water at metal surfaces both in the Ultrahigh Vacuum (UHV) environment and at the metal−liquid interface itself.[2] In the UHV environment, the structure of water at a metal surface depends on the identity of the metal, the amount of water present at the interface, and the presence of any additional adsorbates, such as halides or other anions.[2] On metal surfaces, such as Pt, Ag, Au, and even some faces of Cu, water adsorbs molecularly.[3] The structure of this water depends on the identity of the metal. For example, water forms a "bilayer" on Pt(111) wherein water in the first layer bonds to the metal surface through lone pair electrons donated by the oxygen. A second layer of water is hydrogen bonded to the first with one hydrogen oriented perpendicular to the surface.[2,3] Subsequent layers of water ("multilayers") may be disordered. However, on metals, such as Ag and Au, water is weakly adsorbed and does not form the ordered structure seen on surfaces such as Pt, Ni, and Ru.[2−6] The water structure at the surface of metals, such as Ag and Au, at the gas−solid interface reflects the interplay between the relatively weak H_2O−surface interaction and the relatively strong H_2O−H_2O interaction,[2] resulting in a water structure with little correlation to the surface. In the case of Au and Ag, the surface corrugation

(either physical or electronic) is not sufficient to inhibit surface diffusion, and the water−water interaction energy is comparable to the water−metal interaction energy.[2]

The condensed phase electrochemical environment differs from that present in UHV studies in a number of important particulars. The temperature of the condensed phase interface is typically at room temperature, while that in UHV is of necessity at temperatures below water desorption, which occurs between 130 and 250 K. Additionally, the electrochemical environment is complicated by the presence of electrolyte and applied potential.

At the electrochemical interface, the higher temperatures relative to the gas−solid work and the presence of electrolyte and excess solvent complicate surface solution interactions. In the electrochemical environment, interfacial structure is described by the Gouy−Chapman−Stern (GCS) theory, which has been used to model differential capacity measurements. Specific predictions of this theory with regard to the potential dependence of the capacity only hold at potentials near the pzc before breaking down. GCS theory fails to account for ion−ion correlations, strong nonspecific interactions of ions with surface charge, and variation with applied potential that will all affect the capacitance of the double layer.[7] Discrepancies between the theory and experimentally measured capacity have also long been ascribed to the presence of an organized H-bonded layer of H_2O at the interface.[8] More recent models that include different ion interactions demonstrate improved ability to reproduce the observed electrochemical response.[9−11] It has long

(1) Menzel, D. *Science* **2002**, *295*, 58−59.
(2) Henderson, M. A. *Surf. Sci. Rep.* **2002**, *46*, 1−308.
(3) Thiel, P. A.; Madey, T. F. *Surf. Sci. Rep.* **1987**, *7*, 211−385.
(4) Ikemiya, N.; Gewirth, A. A. *J. Am. Chem. Soc.* **1997**, *119*, 9919−9920.
(5) Su, X.; Lianos, L.; Shen, Y. R.; Somorjai, G. A. *Phys. Rev. Lett.* **1998**, *80*, 1533−1536.
(6) Morgenstern, K.; Nieminen, J. *Phys. Rev. Lett.* **2002**, *88*, 066102/1−066102/4.
(7) Bard, A. J.; Faulkner, L. R. *Electrochemical Methods: Fundamentals and Applications*, 2nd ed.; John Wiley & Sons: New York, 2001.
(8) Parsons, R. *Chem. Rev.* **1990**, *90*, 813−826.
(9) Fawcett, W. R.; Smagala, T. G. *J. Phys. Chem. B* **2005**, *109*, 1930−1935.
(10) Boda, D.; Henderson, D.; Plaschko, P.; Fawcett, W. R. *Mol. Simul.* **2004**, *30*, 137−141.
(11) Andreu, R.; Fawcett, W. R. *J. Electroanal. Chem.* **2003**, *552*, 105−110.

been understood that water is organized around ions in solution,[12] a point emphasized in recent gas-phase cluster measurements[13,14]

There have been a number of studies directly examining the structure of water at the electrified metal−liquid interface. Toney and co-workers used X-ray reflectivity to show that oxygen distributions for water at the Ag(111) surface changed at potentials on either side of the pzc. This result was interpreted to suggest that water molecules exhibited different orientations depending on surface charge.[15] Ataka et al. used surface enhanced IR absorption spectroscopy (SEIRAS) to examine potential dependent changes in the bending modes of water that confirmed water reorientation on different sides of the pzc on Au(111) in $HClO_4$ electrolyte.[16] Iwasita ascribed IR intensity changes in the OH stretches on a Pt(111) surface to the inversion of water as the potential was scanned past the pzc.[17] Additionally, STM measurements have long reported evidence for a condensed ($\sqrt{3} \times \sqrt{7}$) phase, likely consisting of a 1:1 bisulfate/water layer at potentials positive of the pzc on many (111) faces of fcc materials.[18−26] More recently, infrared visible sum frequency generation (SFG) spectroscopy has examined the OH stretches on polycrystalline Au with specific reference to the water reorientation question.[27] Two reports using SFG to examine the OD stretch in D_2O-containing solutions also address the potential dependent water structure at a Pt surface.[28,29] However, there is still little understanding concerning the exact nature of the structure of water at the electrified metal interface, the relationship of this structure to that found in UHV, and the role of electrolyte in altering or controlling this structure.

Vibrational spectroscopy could, in concept, provide considerable insight into the structure of water at the electrified interface, and indeed, it has a major role in developing the understanding described above. Traditional vibrational spectroscopies are often hampered by their inability to discriminate interfacial water structure from that present in the bulk above the interface.[2] In this paper, we use interface specific, in situ SFG to examine the structure of water at the Ag−water interface with and without electrolyte. In SFG spectroscopy, the signal arises from the broken symmetry present at the interface, which eliminates complicating contributions from bulk H_2O above the surface.[30−33] SFG studies of nonconducting surfaces in solution, such as quartz, sapphire, and CaF_2, have shown that the orientation of H_2O molecules is highly sensitive to the charge present at the interface.[34−36] Molecules, such as CH_3CN, H, CO, and CN^-, have been observed by SFG spectroscopy at the electrochemical interface.[29,31] Interestingly, the vibrational mode of under potential deposited hydrogen on Pt is influenced by hydrogen bonding to water.[37] However, there are no reports examining the OH stretch above the well-defined single-crystal metal surface in the electrochemical environment. This lack of information is in contrast to the detailed picture of water emerging at the liquid−liquid or the liquid−insulator interface, where the exquisite environmental sensitivity of the OH stretch is utilized to report on water structure. In this paper, we address the structure of water at the electrified metal−liquid interface by using the surface sensitivity of SFG spectroscopy to probe the fundamental OH stretching mode of H_2O at the Ag(100)−solution interface. Because these measurements are performed with the metal surface in the electrochemical environment, we can examine the response of this stretching mode in the presence of electrolyte, solvent, and applied potential.

2. Experimental Section

For this study, the silver surface was a Ag(100) single crystal (Monocrystals Co.), whose orientation was confirmed by Laue' X-ray backscattering. The crystal was polished to mirror finish using progressively finer grit Al_2O_3 powders or diamond suspensions (Buehler Metadi Supreme) followed by a chemical polish using a CrO_3 solution.[38] Following the chemical polish, the crystal was maintained in water (Milli-Q UV-Plus, 18.2 $M\Omega$ cm^{-1}) to prevent oxidation of the surface. The electrolyte solution was either 0.1 M KF or 0.1 M NaF (Alfa Aesar, Puratronic 99.995%). Isotopic substitution was performed using D_2O (Aldrich 99.9% isotopically enriched). The solution was bubbled with argon for at least 30 min to remove residual oxygen, prior to filling the spectroelectrochemical cell. A Au wire was used for the counter electrode, and potentials were measured relative to a Ag/AgCl reference electrode. All potentials stated are reported relative to this Ag/AgCl reference. Hexane thiol monolayers were prepared by soaking a Ag(111) surface in a solution of 10 mM hexane thiol (Aldrich) in ethanol overnight. The monolayers were rinsed with ethanol and water prior to immersion in the spectroscopy cell.

Cyclic voltammetry (CV) and differential capacitance measurements were obtained in a two-compartment glass cell with a Au wire counter electrode and a Ag/AgCl reference electrode. CV was performed using a 50 mV/s scan rate. Capacitance measurements were obtained with an excitation of frequency 10 Hz and an amplitude of 5 mV at a 7 mV/s scan rate.

The details of our cell[39] and SFG spectrometer[40] have been previously reported. Briefly, the visible and infrared beams are arranged in a co-

(12) Conway, B. E. *Phys. Chem.* **1970**, *9A*, 1−166.
(13) Weber, J. M.; Kelley, J. A.; Nielsen, S. B.; Ayotte, P.; Johnson, M. A. *Science* **2000**, *287*, 2461−2463.
(14) Ayotte, P.; Nielsen, S. B.; Weddle, G. H.; Johnson, M. A.; Xantheas, S. S. *J. Phys. Chem. A* **1999**, *103*, 10665−10669.
(15) Toney, M. F.; Howard, J. N.; Richer, J.; Borges, G. L.; Gordon, J. G.; Melroy, O. R.; Wiesler, D. G.; Yee, D.; Sorensen, L. B. *Nature* **1994**, *368*, 444−446.
(16) Ataka, K.-i.; Yotsuyanagi, T.; Osawa, M. *J. Phys. Chem.* **1996**, *100*, 10664−10672.
(17) Iwasita, T.; Xia, X. *J. Electroanal. Chem.* **1996**, *411*, 95−102.
(18) Edens, G. J.; Gao, X.; Weaver, M. J. *J. Electroanal. Chem.* **1994**, *375*, 357−366.
(19) Magnussen, O. M.; Hageboeck, J.; Hotlos, J.; Behm, R. J. *Faraday Discuss.* **1992**, *94*, 329−338.
(20) Nishizawa, T.; Nakada, T.; Kinoshita, Y.; Miyashita, S.; Sazaki, G.; Komatsu, H. *Surf. Sci.* **1996**, *367*, L73−L78.
(21) Wan, L.-J.; Yau, S.-L.; Itaya, K. *J. Phys. Chem.* **1995**, *99*, 9507−9513.
(22) Wan, L.-J.; Hara, M.; Inukai, J.; Itaya, K. *J. Phys. Chem. B* **1999**, *103*, 6978−6983.
(23) Wan, L. J.; Suzuki, T.; Sashikata, K.; Okada, J.; Inukai, J.; Itaya, K. *J. Electroanal. Chem.* **2000**, *484*, 189−193.
(24) Funtikov, A. M.; Linke, U.; Stimming, U.; Vogel, R. *Surf. Sci.* **1995**, *324*, L343−L348.
(25) Funtikov, A. M.; Stimming, U.; Vogel, R. *J. Electroanal. Chem.* **1997**, *428*, 147−153.
(26) Wilms, M.; Broekmann, P.; Stuhlmann, C.; Wandelt, K. *Surf. Sci.* **1998**, *416*, 121−140.
(27) Nihonyanagi, S.; Ye, S.; Uosaki, K.; Dreesen, L.; Humbert, C.; Thiry, P.; Peremans, A. *Surf. Sci.* **2004**, *573*, 11−16.
(28) Zheng, W.; Tadjeddine, A. *J. Chem. Phys.* **2003**, *119*, 13096−13099.
(29) Baldelli, S.; Mailhot, G.; Ross, P. N.; Somorjai, G. A. *J. Am. Chem. Soc.* **2001**, *123*, 7697−7702.
(30) Bain, C. D. *J. Chem. Soc., Faraday Trans.* **1995**, *91*, 1281−1296.
(31) Tadjeddine, A.; Peremans, A. *J. Electroanal. Chem.* **1996**, *409*, 115−121.
(32) Shultz, M. J.; Schnitzer, C.; Simonelli, D.; Baldelli, S. *Int. Rev. Phys. Chem.* **2000**, *19*, 123−153.
(33) Richmond, G. L. *Chem. Rev.* **2002**, *102*, 2693−2724.
(34) Becraft, K. A.; Moore, F. G.; Richmond, G. L. *Phys. Chem. Chem. Phys.* **2004**, *6*, 1880−1889.
(35) Yeganeh, M. S.; Dougal, S. M.; Pink, H. S. *Phys. Rev. Lett.* **1999**, *83*, 1179−1182.
(36) Du, Q.; Freysz, E.; Shen, Y. R. *Phys. Rev. Lett.* **1994**, *72*, 238−241.
(37) Peremans, A.; Tadjeddine, A. *Phys. Rev. Lett.* **1994**, *73*, 3010−3013.
(38) Hamelin, A.; Doubova, L.; Stoicoviciu, L.; Trasatti, S. *J. Electroanal. Chem. Interfacial Electrochem.* **1988**, *244*, 133−145.
(39) Schultz, Z. D.; Biggin, M. E.; White, J. O.; Gewirth, A. A. *Anal. Chem.* **2004**, *76*, 604−609.
(40) Mani, A. A.; Dreesen, L.; Hollander, P.; Humbert, C.; Caudano, Y.; Thiry, P. A.; Peremans, A. *Appl. Phys. Lett.* **2001**, *79*, 1945−1947.
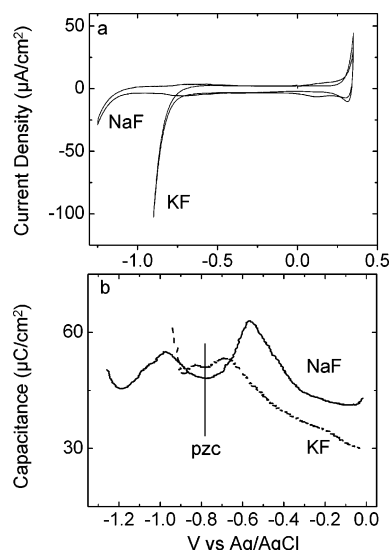
Figure 1. (a) CV and (b) differential capacitance obtained from a Ag(100) surface in a solution containing either 0.1 M NaF or 0.1 M KF as indicated. The pzc of Ag(100) is denoted by the line in the differential capacitance measurement.

propagating geometry incident to the sample normal at 55 and 65°, respectively. The spectroelectrochemical cell consists of a glass/Kel-F body sealed by a 60° equilateral CaF_2 prism. The prism is sealed to the Kel-F base by means of a Teflon-coated O-ring. The single-crystal electrode is attached to a glass/Kel-F plunger and pressed against the prism to minimize beam attenuation due to solvent. The solution layer thickness is estimated to be between 1 and 10 μm. Spectra were acquired with the ppp laser beam polarization combination. To account for variation in laser power, each SFG spectrum was simultaneously normalized to the infrared power.

The intensity of the SFG response can be modeled, as shown in eq 1.[33]

$$I_{SF} \propto \left| \chi_{NR} \times e^{i\varphi_n} + \sum_n \frac{A_n}{\omega_{IR} - \omega_n + i\Gamma_n} \right|^2 \tag{1}$$

In eq 1, χ_{NR} corresponds to the nonresonant electronic contributions and is fit as a constant. ω_{IR} is the energy of the tuned infrared power. Vibrational modes are modeled as a sum of n Lorentz-type functions with intensity A_n, energy ω_n, and a damping coefficient Γ_n. φ_n represents the difference between the nonresonant phase and the phase of the vibrational modes. Fitting was accomplished using routines developed at the University of Illinois as well as that obtained from Dr. Lee Richter (NIST). In our fits, there was no clear feature negative of the baseline to accurately account for interference between the nonresonant and resonant signals, so a common phase angle (φ) for each resonance was used in our model. SFG spectra of alkane thiols on Ag were adequately fit by eq 1. SFG spectra in the OH stretching region exhibited a large inhomogeneous broadening component. To compensate for this additional broadening in the water spectra, the Lorentz profile was convoluted with a Gaussian intensity distribution in a manner similar to previous reports.[30,33]

3. Results

3.1. Electrochemical Results. Figure 1 shows the CV and differential capacitance measurements for Ag(100) in 0.1 M KF and 0.1 M NaF electrolytes. In Figure 1a, the CV shows the oxidation and dissolution of Ag at potentials positive of 0.2 V for both electrolytes. Upon reversing the potential scan direction, there is a small negative peak corresponding to the re-reduction
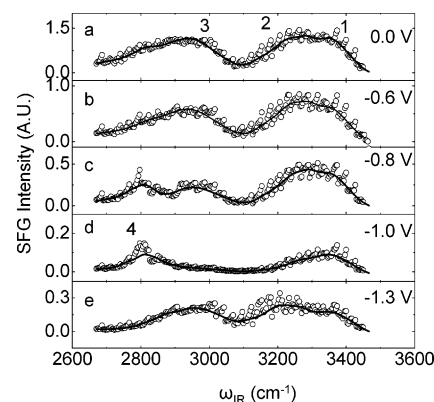
Figure 2. Potential dependent SFG spectra obtained from a Ag(100) surface in 0.1 M NaF at (a) 0.0 V, (b) −0.6 V, (c) −0.8 V, (d) −1.0 V, or (e) −1.3 V. Peak labels and potentials are indicated. Solid lines are the fitting result.
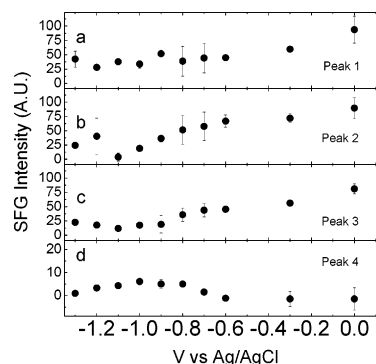

Figure 3. Peak intensity versus potential for (a) peak 1, (b) peak 2, (c) peak 3, and (d) peak 4, all obtained from a Ag(100) surface in a solution of 0.1 M NaF.

of Ag^+ back to Ag metal. At cathodic potentials, the onset of H_2 gas evolution is observed at a potential of −0.85 V in 0.1 M KF and −1.15 V in 0.1 M NaF. There are no other features present in the voltammogram, consistent with earlier reports.[41] In Figure 1b, differential capacitance obtained from both electrolytes exhibits a minimum at 0.8 V (marked with a line), indicating the potential of zero charge (pzc). The pzc is found near the potential of hydrogen evolution for the KF solution, as evidenced by the sharp rise in the capacity at more negative potentials. The pzc obtained here agrees with values previously reported for the Ag(100) surface.[42]

3.2. SFG from Ag(100) with Electrolyte. Figure 2 shows the potential dependent SFG spectra obtained using a Ag(100) single crystal in a solution containing 0.1 M NaF. The spectra in Figure 3 were obtained over a potential range (0.0 to −1.3 $V_{Ag/AgCl}$) selected to avoid oxidation of the Ag surface at positive potentials and to avoid evolution of large amounts of hydrogen gas at negative potentials as determined by CV. Fitting analysis indicates the presence of peaks at 3370 (peak 1), 3250 (peak 2), and 2970 (peak 3) cm^{-1}. As the potential is made negative, the intensities are observed to diminish. As the potential approaches the pzc, a fourth feature is observed at 2800 cm^{-1} (peak 4). SFG spectra obtained in 0.1 M KF (Supporting Information) exhibit the same peaks, with similar potential dependent behavior. SFG spectra obtained from Ag(111) in 0.1

(41) Valette, G.; Hamelin, A. *J. Electroanal. Chem. Interfacial Electrochem.* **1973**, *45*, 301−319.
(42) Valette, G. *J. Electroanal. Chem. Interfacial Electrochem.* **1987**, *224*, 285−294.

M NaF also evince the same peaks (Supporting Information). Peaks 1 and 2 exhibiting similar behavior were observed above a disordered Au surface in acid solution in SFG obtained in the ATR configuration.[27]

SFG contributions from the CaF_2 window–solution interface were determined to be negligible by backing the crystal away from the cell window and observing the signal go to zero, in agreement with previously reported results at this pH.[29,34] At other pH values, CaF_2 evinces a substantial signal from water that must be accounted for in the thin layer configuration.[34] The potential dependence of the observed peaks additionally suggests that the molecules interrogated by SFG are associated with the electrode surface. Since the CV measurements indicate no redox activity over the potential region interrogated here, the composition of the bulk solution does not change with applied potential. At the electrolyte concentrations used, the Debye length is 0.96 nm.[7] This length is 3 orders of magnitude smaller than the gap between the electrode and the prism in our thin layer configuration. Changes observed in the resonant portion of the SFG spectrum must be related to changes in molecular behavior at the electrode surface.

The observed SFG response is the product of the Fresnel coefficients and the nonlinear susceptibility. In the region between 3000 and 3800 cm^{-1}, the infrared absorption of bulk water makes the Fresnel coefficients low and depend intimately on the separation between the Ag crystal and the CaF_2 prism. These low Fresnel coefficients make detailed analysis of line shape challenging in this wavelength region. Increased dispersion in the absorption region may influence the observed line shape of peaks 1 and 2. However, the Fresnel coefficients are insensitive to applied potential. Thus for a given crystal–prism distance and experimental setup, potential dependent changes in the SFG must be associated with changes in the nonlinear susceptibility and thus interfacial molecules. The observation of potential dependent SFG shows that the observed bands 1–4 are not artifacts arising from the low Fresnel coefficients in this spectral region.

The potential dependent SFG peak intensities for Ag(100) in 0.1 M NaF are plotted in Figure 3. In Figure 3, the intensities of peaks 2 and 3 show monotonic decreases as the potential is made negative. The intensity of peak 1 shows a small decrease in intensity as the potential is scanned negatively. The intensity behavior of peak 1 could also be described to remain constant over much of the potential region showing only a slight increase at positive potentials. At potentials just negative of the pzc, only peaks 1 and 4 show substantial intensity. As the potential is made sufficiently negative, the spectra again exhibit increasing contributions from peaks 2 and 3. The potential dependence of peak 4 in 0.1 M NaF shows interesting behavior. At potentials near the pzc, peak 4 is observed to increase and persist until −1.2 V, where it shows a marked decrease in intensity. The potential dependence in 0.1 M KF (Figure 4) is similar to that in NaF; however, the onset exhibits decreased intensity relative to that in NaF electrolyte.

H_2 gas evolution (vide supra) at a less negative potential precludes investigation at potentials substantially negative of the pzc. In NaF electrolyte, peak 4 is prominent at potentials negative prior to H_2 gas evolution. In KF electrolyte, peak 4 is observed, but at less than 50% the intensity observed with NaF.
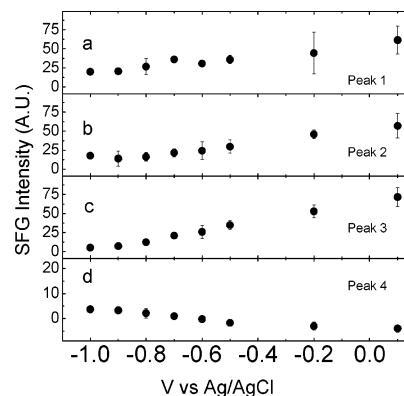

Figure 4. Peak intensity versus potential for (a) peak 1, (b) peak 2, (c) peak 3, and (d) peak 4, all obtained from a Ag(100) surface in a solution of 0.l M KF.
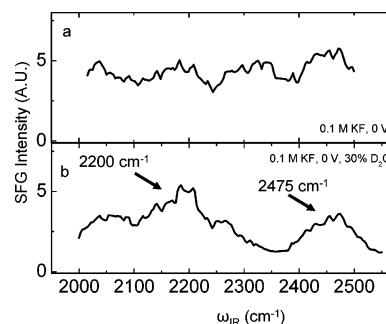

Figure 5. SFG spectra from 2000–2550 cm^{-1} obtained from a Ag(100) surface in (a) 0.1 M KF in H_2O and (b) with 30% D_2O added at 0.0 V.

3.3. SFG in D_2O-Containing Solution. The features in the SFG spectra were confirmed to arise from the OH stretches by isotope substitution, as shown in Figure 5. Figure 5a is the SFG spectrum obtained in the spectral region between 2000 and 2500 cm^{-1} in H_2O + 0.1 M KF at 0.0 V. This spectrum exhibits a flat response, as expected. At this point, the crystal was retracted, potential control maintained, and sufficient D_2O added to the cell to give approximately 30% D_2O. The SFG spectrum obtained immediately following at 0.0 V (Figure 5b) exhibits two broad features centered at 2200 and 2475 cm^{-1}. Using the isotope factor of 1.35, these features correspond to modes at 2970 and 3341 cm^{-1}, in agreement with the features seen at higher energy in H_2O.

3.4. SFG from a Thiol-Modified Ag(111) Surface. Figure 6 shows the SFG spectrum obtained from a Ag(111) surface decorated with a monolayer of hexanethiol in 0.1 M NaF. Thiols are known to form well-packed monolayers on Ag(111) surfaces.[43] Figure 6a shows that addition of the thiol to the Ag surface yields five new bands in the region between 2800 and 3000 cm^{-1}, a blow-up of which is given in the inset. Additionally, the SFG spectrum exhibits broad features in the energy region corresponding to peaks 1 and 2, described above. The inset to Figure 6a also shows the fit to eq 1 for the thiol region. This fit was accomplished using only modes corresponding to the thiol. These modes arise from both methyl and methylene stretches of the adsorbed molecule.[44] From the fit, the energies of the modes are 2852, 2878, 2920, 2935, and 2968 cm^{-1}, in exact agreement with previous reports.[44] The magnitude of the

(43) Laibinis, P. E.; Whitesides, G. M.; Allara, D. L.; Tao, Y. T.; Parikh, A. N.; Nuzzo, R. G. *J. Am. Chem. Soc.* **1991**, *113*, 7152–7167.
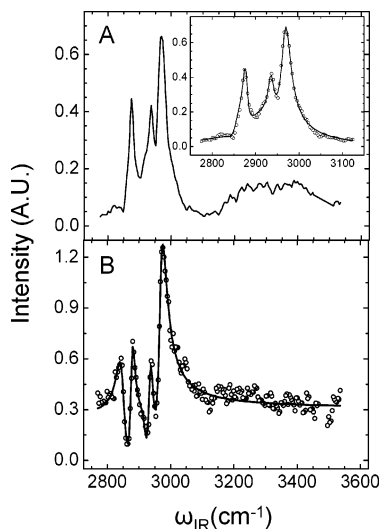(44) Potterton, E. A.; Bain, C. D. *J. Electroanal. Chem.* **1996**, *409*, 109–114.

Figure 6. SFG spectra obtained from a thiol-decorated Ag(100) surface in 0.1 M NaF in (a) H_2O and (b) D_2O. Solid lines are the fitting result. Inset shows the fit for the thiol region of a.

nonresonant background was found to be nearly zero. This spectrum exhibited little potential dependence over a region between 0.2 and −0.7 V, consistent with the nearly potential-independent capacity found for thiol systems in this potential range.[45,46] At potentials outside this range, thiol desorption and oxidation is known to occur.[46,47] The presence of the thiol results in the disappearance of features associated with peaks 3 and 4 observed on the bare Ag surface.

Figure 6b shows the SFG spectrum obtained from a hexane thiol monolayer on Ag(111) in a solution containing 0.1 M NaF in D_2O. There are two major changes in Figure 6b relative to the spectrum obtained in H_2O in Figure 6a. First, the OH stretching modes observed in Figure 6a are no longer present. Second, the thiol peaks in D_2O-containing solution appear as derivatives, rather than peaks. The origin of the derivative shape is ascribed to interference between the resonant and nonresonant components of the SFG signal and has been reported previously for Ag surfaces.[30,48] The solid line in Figure 6b is the result of fitting the spectrum to eq 1. The energy of the peaks obtained from this fit matched exactly those found from the fit to the spectrum in Figure 6a. However, the spectrum obtained from D_2O-containing solution required a significant nonresonant component in the fit.

4. Discussion

The results given above show that the bare Ag surface exhibits four peaks in the OH stretching region, the intensities of which exhibit potential dependence. These peaks are associated with H_2O on the basis of their sensitivity to isotopic substitution. These peaks do not arise from the CaF_2−solution interface, in agreement with previous results for water at this pH.[34] Additionally, passivating the Ag surface with an alkanethiol results in the disappearance of the two low-energy OH stretches observed on the bare surface. The observation of four peaks

associated with OH stretches speaks to water molecules in different environments.

4.1. Assignment of Peaks 1−4. The energy of an OH stretch from H_2O is associated with the environment experienced by the molecule. A higher degree of hydrogen bonding lowers the energy of the OH stretch.[49] In the OH stretch region, liquid water exhibits a broad envelope between 3000 and 3700 cm^{-1}, which is typically deconvoluted into stretches at 3620 and 3435 cm^{-1} and sub-bands at 3540 and 3240 cm^{-1} attributed to the overlap of bending overtones with these two stretches.[49] Intermolecular coupling makes interpretation complicated, and these modes remain the focus of research.[50] The vibrational modes of amorphous solid water in this region are an antisymmetric OH stretch at 3253 cm^{-1}, a symmetric stretch at 3191 cm^{-1}, and a combination of the symmetric stretch and a lattice mode at 3367 cm^{-1}.[49] Ice (I_h) exhibits modes at 3080, 3420, 3210, and 3320 cm^{-1} assigned to symmetric in-phase, symmetric out-of-phase, and antisymmetric TO−LO splitting modes, respectively.[51] At an interface, modes located between 3100 and 3500 cm^{-1} are commonly assigned to OH stretches of hydrogen-bonded water.[52]

4.1.1. Peak 1. On the basis of the correlation between the band observed at 3370 cm^{-1} in our spectrum and the symmetric OH stretch in liquid water at 3435 cm^{-1}, we associate peak 1 with water exhibiting the degree of hydrogen bonding similar to that found in liquid. This correlation is common in the SFG literature.[33,36] The energy of peak 1 suggests that the water associated with this OH stretch exhibits a low level of hydrogen bonding and weakly interacts with the Ag surface. In UHV, a band at 3390 cm^{-1} observed in HREELS measurements was ascribed to disorganized and weakly adsorbed water on a Ag(100) surface.[53] Independent low-temperature STM measurements in UHV of H_2O adsorbed on Ag(111) confirm the presence of a disordered water adlayer at low water coverage.[6]

Peak 1 exhibits only a weak potential dependence, with possibly higher intensity at the most positive potentials examined here. Additionally, intensity in the energy region of peak 1 was also observed when access to the Ag surface was restricted by the thiol monolayer. This indicates peak 1 is associated with water found in the solution above the surface. On the basis of this, we associate peak 1 with disorganized "liquidlike" water above the Ag surface in the diffuse double layer region.

4.1.2. Peak 2. Peak 2 is observed at an energy that is commonly associated with water hydrogen bonded in a tetrahedral manner similar to that found in ice.[36] "Icelike" modes in water observed by SFG at other interfaces show marked intensity changes related to the concentration of ions and the resulting interfacial potential.[54] In previous work, this mode is ascribed to water which solvates ionic species at the interface. In our results, the intensity of peak 2 decreases as the potential moves toward the pzc, which is where the surface excess of both cations and anions is at a minimum. The intensity of peak 2 recovers on either side of the pzc, albeit less significantly on the negative

(45) Kabasawa, A.; Matsuda, N.; Sawaguchi, T.; Matsue, T.; Uchida, I. *Denki Kagaku oyobi Kogyo Butsuri Kagaku* **1992**, *60*, 986−991.
(46) Widrig, C. A.; Chung, C.; Porter, M. D. *J. Electroanal. Chem. Interfacial Electrochem.* **1991**, *310*, 335−359.
(47) Hatchett, D. W.; Uibel, R. H.; Stevenson, K. J.; Harris, J. M.; White, H. S. *J. Am. Chem. Soc.* **1998**, *120*, 1062−1069.
(48) Hines, M. A.; Todd, J. A.; Guyot-Sionnest, P. *Langmuir* **1995**, *11*, 493−497.

(49) Rice, S. A. *Top. Curr. Chem.* **1975**, *60*, 109−200.
(50) Rey, R.; Moller, K. B.; Hynes, J. T. *Chem. Rev.* **2004**, *104*, 1915−1928.
(51) Whalley, E. *Can. J. Chem.* **1977**, *55*, 3429−3441.
(52) Du, Q.; Superfine, R.; Freysz, E.; Shen, Y. R. *Phys. Rev. Lett.* **1993**, *70*, 2313−2316.
(53) Ding, X.; Garfunkel, E.; Dong, G.; Yang, S.; Hou, X.; Wang, X. *J. Vac. Sci. Technol. A* **1986**, *4*, 1468−1470.
(54) Gurau, M. C.; Kim, G.; Lim, S.-m.; Albertorio, F.; Fleisher, H. C.; Cremer, P. S. *ChemPhysChem* **2003**, *4*, 1231−1233.

side due to the restricted potential range available before hydrogen evolution. Interestingly, peak 2 is observed nearly independent of potential on the thiol-modified surface, consistent with the Helmholtzian double layer model invoked for this interface.[46]

4.1.3. Peak 3. The low-energy peak 3 also is associated with the OH stretch of H_2O, but from H_2O in an environment different from that of peaks 1 and 2. Surface hydroxide modes are found at energies above 3600 cm^{-1},[34,55] too high in energy for peak 3. The lower energy of peak 1 must arise from a mechanism whereby electron density is removed from the O−H bond. Isotopic substitution measurements confirm the association of this mode with water.

Water-related bands at this low energy have been observed previously. Morgenstern and Nieminen used Inelastic Electron Tunneling Spectroscopy (IETS) at low temperature to interrogate monolayer water adsorbed on Ag(111). They found a broad peak centered at 2900 cm^{-1}—equivalent to peak 3 in the SFG spectrum reported here—which was ascribed to an "anomalous" OH stretch. The origin of this band in the IETS remains unclear, but the authors suggested that the high field attendant the IETS measurement may be at least partly responsible.[6] Gas phase cluster work shows that H_2O solvated around a F^- anion will exhibit a peak at 2900 cm^{-1}, depending on the number of H_2O molecules (and hence the degree of hydrogen bonding) in the solvation shell.[56] Interestingly, Ostroverkhov et al. recently reported the existence of a broad peak at ~3000 cm^{-1} on quartz surface in aqueous solution.[57] They assigned this peak to water hydrogen bonding with surface SiO^- groups.

On the basis of these previous results and the disappearance of the peak when the Ag surface is decorated with thiols, we ascribe peak 3 to water specifically adsorbed to the Ag surface. Specific adsorption of water to Ag would result in removal of electron density from the OH bond and lower the energy of the OH stretch, consistent with the effect observed on quartz.

The potential dependence of the energy of peak 3 is similar to that found for peak 2 in that its intensity is at a minimum at the pzc, but increases to either side. Theory indicates that H_2O associates with a Ag surface absent an applied field in a parallel orientation through electron donation from the oxygen lone pair electrons.[58,59] OH stretches from H_2O so oriented would be IR and SFG inactive. However, when applied potential is included, electrostatic effects dominate water orientation[58] as is also understood from capacity measurements.[8] The field dependence of peak 3 suggests that this peak is associated with H_2O bound to the Ag surface and oriented by the electrolyte and/or the applied field. Near the pzc, the lower intensity of peak 3 is ascribed to the lower field (originating from the lower surface excess of charged species), which corresponds to water with a smaller dipole component normal to the surface (i.e., O−H bonds more parallel to the surface). We note that several studies indicate that water reorients as the potential passes through the pzc, so a parallel orientation is expected at some point.[15−17]

SFG is sensitive to the orientation of molecules at the interrogated interface. In the present case, the absence of a strong nonresonant signal or other phase reference[57] makes the water orientation difficult to definitively assign.

4.1.4. Peak 4. Peak 4 observed at potentials near the pzc is at an energy previously associated with hydronium cation, H_3O^+.[60] The presence of this peak at potentials at or negative of the pzc is expected as the surface becomes more negatively charged. At the onset of H_2 evolution in NaF, the intensity of peak 4 is observed to decrease, presumably because hydronium is consumed in the hydrogen evolution reaction. At equivalent potentials, peak 4 is observed with greater intensity in NaF electrolyte than in KF. The origin of this behavior likely relates to the more facile hydrogen evolution observed in the voltammetry with KF relative to NaF. The increased overpotential for hydrogen evolution found in NaF suggests that Na^+ acts to inhibit hydrogen reduction. The smaller Na^+ cation may better compete with the hydronium for surface sites, relative to K^+. Hydronium is consumed more readily in KF relative to NaF at a given negative potential. In either case, at the solution pH (~6.5) of our experiments, hydronium is not expected to be a major species as reflected by the low overall intensity of this peak.

A peak at similar energy was observed by Friedrich et al. using SFG in acidic solution on Pt; however, they did not report an assignment for this band.[61] In their study, these authors also used a CaF_2 window, and the large interfacial water signal attendant the window−acid solution interface[34] would complicate interpretation of their results.

4.2. Thiol-Decorated Ag Surface. The SFG spectra obtained from the thiol-decorated Ag surface are remarkable for several reasons. First, these spectra obtained in water show that peak 3 must relate to a surface-adsorbed water species since it is absent in spectra obtained from the thiol surface. The presence of peaks 1 and 2 suggests that these bands are associated with the diffuse double layer above the surface. The SFG spectra obtained in D_2O show that peaks 1 and 2 are related to H_2O since they are absent in D_2O. The potential independence of the SFG spectra obtained from the thiol is expected based on the known low and flat capacity of thiol-modified surfaces.[46]

The other remarkable feature in the SFG spectra of the thiol-modified Ag surface relates to the degree of nonresonant background obtained in H_2O and D_2O. The SFG spectra of the thiol-decorated Ag surface obtained in H_2O solution show a surprising lack of nonresonant background, with no features negative of the baseline. This is in contrast to ex situ results reported from thiol-modified Ag surfaces, the spectra from which exhibit derivative looking features.[44] However, in D_2O-containing electrolyte, the expected derivative features are also observed, and the D_2O spectra demonstrate a substantially higher level of nonresonant background equivalent to that found in the ex situ measurement.

In our system, replacing H_2O with D_2O results in higher transmission of infrared intensity to the Ag surface since D_2O is essentially transparent in the spectral region between 2800 and 3500 cm^{-1}. In eq 1, however, changing the IR intensity is insufficient to describe changes in the relative contribution of

(55) Itoh, T.; Sasaki, Y.; Maeda, T.; Horie, C. *Surf. Sci.* **1997**, *389*, 212−222.
(56) Robertson, W. H.; Diken, E. G.; Price, E. A.; Shin, J.-W.; Johnson, M. A. *Science* **2003**, *299*, 1367−1372.
(57) Ostroverkhov, V.; Waychunas, G. A.; Shen, Y. R. *Phys. Rev. Lett.* **2005**, *94*, 046102/1−046102/4.
(58) Sanchez, C. G. *Surf. Sci.* **2003**, *527*, 1−11.
(59) Ranea, V. A.; Michaelides, A.; Ramirez, R.; Verges, J. A.; de Andres, P. L.; King, D. A. *Phys. Rev. B: Condens. Matter Mater. Phys.* **2004**, *69*, 205411/1−205411/9.
(60) Ataka, K.-i.; Osawa, M. *Langmuir* **1998**, *14*, 951−959.
(61) Friedrich, K. A.; Daum, W.; Dederichs, F.; Akemann, W. *Z. Phys. Chem.* **2003**, *217*, 527−545.
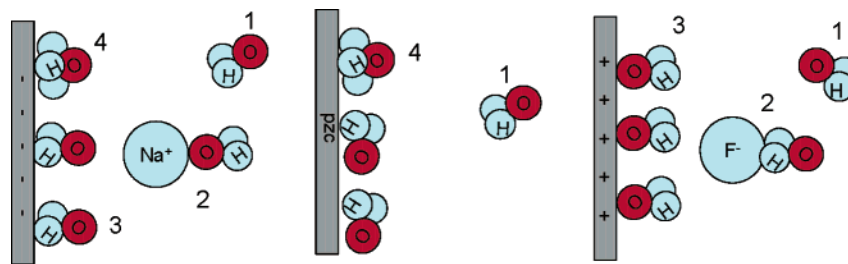
Figure 7. Cartoon depicting water environments associated with peaks observed in the SFG spectra. Numbers indicate associated peak label. The surface charge is positive (right), zero (center), and negative (left).

the resonant and nonresonant components to the SFG signal. Changing the amount of incident IR should attenuate both components equally. In the present system, differential changes in resonant and nonresonant are observed.

Of course, changing from H_2O to D_2O does more than simply change the amount of IR radiation incident on the surface. Other authors have described how changes in the optical system can change the SFG spectral profile from an oscillator near a metal surface. Wilson et al. examined the line profiles arising from a polystyrene/spun-on-glass/Au construct.[62] By manipulating the Fresnel coefficients for several layers close together, the authors were able to adjust the interference between multiple interfaces achieving dips, peaks, and derivative-looking vibrational resonances from the same polystyrene modes. Similar effects achieved by manipulating multiple interfaces were reported by Davies and co-workers.[63,64]

In the present system, the change in transmission between D_2O and H_2O will result in a change in the Fresnel coefficients in the system, which gives rise to the observed interference effects. As in the cases above, there are multiple interfaces present in our system. In other spectral regions on Ag, where IR adsorption by water is not found, we showed recently that a substantial nonresonant background was indeed present.[65] Manipulation of the nonresonant component in the electrochemical environment remains an important challenge.

4.3. Implications for Double Layer Structure. Our results indicate that the electrified metal−solution interface exhibits a diverse assortment of interactions between H_2O, electrolyte ions, and the electrode surface. In particular, there appears to be bands that are surface related and bands that are related to the diffuse double layer region. A model rationalizing our data is shown in Figure 7. At positive potential, electrostatic forces dictate specifically adsorbed H_2O orients oxygen down with a substantial contribution of the molecular dipole normal to the surface. A second H_2O, associated with H_2O solvating anions in the double layer, is observed. A third less H-bonded H_2O is associated with water not interacting with the surface or ions at the interface. Extended order into the diffuse double layer resulting from the applied DC field at the surface is in accord

with previous observations.[33,66] As the applied potential approaches the pzc, the amount of highly hydrogen bonded H_2O, H_2O in the solvation shell of ions, diminishes in the SFG spectrum. The removal of highly hydrogen bonded H_2O is associated with either the lack of charge at the surface or, equivalently, desorption of anions from the surface. The low SFG signal from the covalently bound water (peak 3) likely arises from a change in orientation of the water molecule. As the potential is made further negative of the pzc, both surface-coordinated and ion-solvating water modes are observed to increase in intensity. Hydronium is observed at potentials near the pzc but prior to hydrogen evolution.

The figure shows that water reorients negative of the pzc. Measurements by Osawa[16] and Toney[15] showed that water in electrochemical systems, different from the one examined here, reorients as the potential is moved through the pzc. While our measurements suggest that water adopts a parallel orientation at the electrode surface at the pzc, the data are not yet sufficient to comment on absolute water orientation on either side. However, the increased intensity in peak 3 away from the pzc does suggest that water is orienting with a component normal to the electrode surface in response to potential. The reorientation of water suggested here is consistent with the "flip-flop" model of water developed from SFG measurements at ionic, nonconducting, surfaces.[34−36]

(62) Wilson, P. T.; Briggman, K. A.; Wallace, W. E.; Stephenson, J. C.; Richter, L. J. *Appl. Phys. Lett.* **2002**, *80*, 3084−3086.
(63) Holman, J.; Davies, P. B.; Neivandt, D. J. *J. Phys. Chem. B* **2004**, *108*, 1396−1404.
(64) McGall, S. J.; Davies, P. B.; Neivandt, D. J. *J. Phys. Chem. B* **2004**, *108*, 16030−16039.
(65) Schultz, Z. D.; Gewirth, A. A. *Anal. Chem.* **2005**, in press.

(66) Yan, E. C. Y.; Liu, Y.; Eisenthal, K. B. *J. Phys. Chem. B* **1998**, *102*, 6331−6336.